

Asymmetrically Distorted Structure, Selective Bond Length Alternation, and Reactions of Radical Cations of Silacyclohexanes: An ESR and *ab-Initio* MO Study

Kenji Komaguchi and Masaru Shiotani*

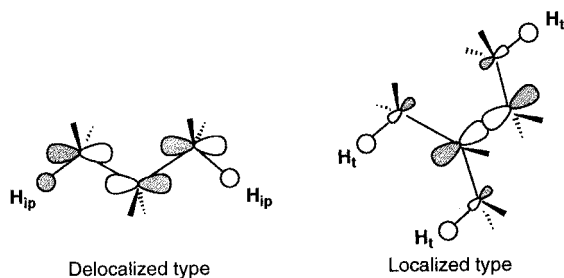
Department of Applied Chemistry, Faculty of Engineering, Hiroshima University,
Higashi-Hiroshima 739, Japan

Received: March 17, 1997; In Final Form: May 20, 1997[⊗]

The structure, dynamics, and thermal reactions of the radical cations of silacyclohexanes (*c*SiC5) containing one Si atom in the six-membered ring have been studied by means of ESR spectroscopy and *ab-initio* MO calculations. The *c*SiC5 radical cations were generated in perfluoromethylcyclohexane matrix by ionization radiation at low temperature. By the help of selectively deuterated or methylated silacyclohexanes the 4.2 K ESR spectrum of *c*SiC5⁺ was successfully analyzed in terms of four different isotropic ¹H hyperfine coupling (hfc) constants: 7.55 mT to the equatorial hydrogen (H_{3e}) at the C(3) position, 3.45 mT to H_{6e}, 2.85 mT to H_{5e}, and 2.60 mT to H_{2e}. The result strongly suggests that the *c*SiC5 radical cation takes an asymmetrically distorted C₁ structure with one of the Si–C bonds elongated in which the unpaired electron mainly resides. *Ab-initio* MO calculations support the distorted structure. A suggested mechanism for the structural distortion is a pseudo-Jahn–Teller effect. Temperature dependent ESR line shapes were observed between 4.2 and 130 K. They were analyzed in terms of the dynamics of two-site jumping between two equivalent and asymmetrically distorted mirror image structures so as to give a selective bond length alternation between two adjacent Si–C bonds. The jumping rate was evaluated to be 12 MHz at a low temperature of 4.2 K and independent of temperatures below 40 K to give a nonlinear Arrhenius plot. The dynamics is suggested to be caused by a quantum mechanical tunneling effect at zero-vibrational levels of a symmetrical double-well potential surface. Furthermore, thermal reactions of *c*SiC5⁺ are presented.

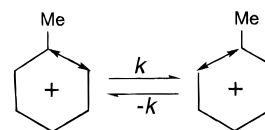
Introduction

The earlier ESR studies of saturated hydrocarbon radical cations have suggested that their electronic structure can be grouped into two types, a delocalized type and a localized type (below), based on the unpaired electron distribution. The former type includes the radical cations of normal alkanes ($n\text{C}_n\text{H}_{2n+2}$, $n \geq 3$) and cycloalkanes ($c\text{C}_n\text{H}_{2n}$, $n \geq 4$) in which the unpaired electron delocalizes over the framework,^{1–4} while the radical cations of branched alkanes, such as 2-methylbutane, belong to the latter type in which the unpaired electron mainly localizes on a particular $\sigma(\text{C}–\text{C})$ bond.^{5,6} It has been also reported that saturated hydrocarbons with a *nondegenerated* HOMO (*i.e.*, Jahn–Teller inactive molecules) can hold their original geometrical symmetry of the precursor neutral molecule after one-electron oxidation.^{1–6}



On the other hand, one of us (M.S.) has reported the electronic structure and dynamics of radical cations of methylcyclohexane (Me-*c*C6) and 1,1-dimethylcyclohexane (1,1-Me₂-*c*C6) by using the low-temperature halocarbon matrix isolation ESR technique.^{7–10} In the papers it has been concluded that those

radical cations take an asymmetrically distorted geometrical structure (²A in C₁) with one of the two C–C bonds elongated, which are attached by methyl group(s). The reversible temperature dependent ESR line shapes were observed between 4.2 and 173 K. They were explained in terms of a selective bond length alternation between the two adjacent C–C bonds.



With increasing temperature, the structural distortions of Me-*c*C6⁺ and 1,1-Me₂-*c*C6⁺ are gradually averaged due to intramolecular dynamics so as to give apparently the same geometrical symmetry of C_s as the neutral molecules. These experimental results imply that the saturated hydrocarbons possessing certain symmetrical elements in the structure such as C_s, C₂, or C_{2v} may decrease in symmetry after one-electron oxidation in spite of being Jahn–Teller inactive molecules. Therefore the delocalized structure cannot be necessarily preferable to the localized one in some σ -radical cations which have so far been regarded as the delocalized type. In the present paper the previous studies on Me-*c*C6⁺ and 1,1-Me₂-*c*C6⁺ were fully extended to the radical cations of silacyclohexane (*c*SiC5), 1-methylsilacyclohexane (1-Me-*c*SiC5), and 1,1-dimethylsilacyclohexane (1,1-Me₂-*c*SiC5), which contain one Si atom in the ring structure. There are several reasons why we are interested in silacycloalkanes. First, since the ionization potential of Si is lower than that of carbon,¹¹ the unpaired electron is expected to predominantly reside on the $\sigma(\text{Si}–\text{C})$ bond(s) of the sila-alkane radical cations such as *c*SiC5⁺. This may lead us to confirm by ESR spectroscopy whether the unpaired electron favorably resides on a particular Si–C bond or on the two Si–C bonds equally,

* Fax: +81-824 24 7736. E-mail: mshiota@ipc.hiroshima-u.ac.jp.

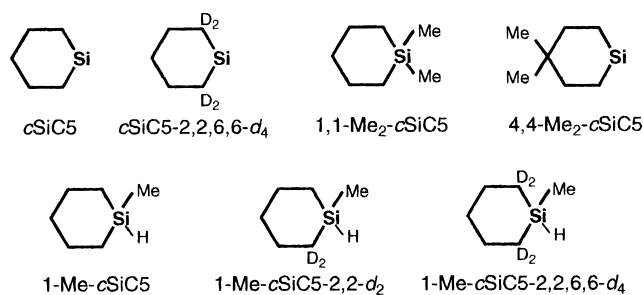
[⊗] Abstract published in *Advance ACS Abstracts*, August 1, 1997.

in other words, whether the *c*SiC5 radical cation has the geometrical structure of asymmetrically distorted C_1 or symmetrical C_3 . Thus, the Si atom can be regarded to play a role as a "probe" to detect the structure distortion. Second, silacyclohexane is known to take a chair structure which is rigid enough in ESR time scale.¹² That is, we do not need to worry about geometrical isomers which make the associated ESR spectra complex as generally observed for linear alkane radical cations.^{1-4,13-16} Third, we can rather easily synthesize the selectively deuterated and methylated silacyclohexanes, which allows us to unambiguously assign the experimental spectra.

We report experimental evidence that the radical cations of silacyclohexanes have an asymmetrically distorted structure in the ground electronic state regardless of matrix used. The results are discussed on the basis of the second-order Jahn–Teller effect by the help of MO calculations. Then, the temperature dependent ESR line shapes are presented and successfully analyzed in terms of a dynamic model of the selective Si–C bond length alternation between two equivalent and asymmetrically distorted mirror image structures. A suggested mechanism for the dynamics is quantum mechanical tunneling at zero-vibrational levels of symmetrical double-well potential surfaces. Furthermore, geoselective thermal deprotonations were observed to convert the ions into neutral radicals depending on not only the matrix used but also whether the two methyl groups are on the Si or not.

Experiment and Calculations

The solute molecules, silacyclohexane (*c*SiC5), and its methyl and/or selectively deuterated derivatives explored in this study are shown below. They were synthesized by the conventional



methods,¹⁷ and the purity of more than 99% was confirmed with ¹H and ¹³C NMR spectra (JEOL Model Ex-270 spectrometer). The substitution ratio of deuterium (D) to H at a certain position in the selectively deuterated compounds was 98%: the ratio is usually governed by the deuterium content of LiAlD₄ (Aldrich Chemical Co., Inc.) used as a reducing reagent. The matrix molecules used are perfluoromethylcyclohexane, CF₃-cC₆F₁₁ (Tokyo Kasei Kogyo Co., Ltd.), and perfluorocyclohexane, cC₆F₁₂ (Aldrich Chemical Co., Inc.), and other halocarbons such as CFCl₃ and CFCl₂CF₂Cl (Tokyo Kasei Kogyo Co., Ltd.). They were used without further purification.

The solid solutions containing *ca.* 0.1 mol % solute molecule in a halocarbon matrix were prepared in Suprasil ESR sample tubes (diameter 4 mm), by several freeze, degas, and thaw cycles on a vacuum line. They were irradiated with γ -rays from ⁶⁰Co with a total dose of *ca.* 1 Mrad at 4.2 or 77 K and subjected to an ESR study. The method is well established to generate solute radical cations and stabilize them in the matrix molecules.¹⁸⁻²⁰ ESR spectra were recorded on Bruker ESP 300E spectrometer from 4.2 K to the temperature at which all solute radicals decayed out. The temperatures were controlled with an Oxford continuous flow cryostat, ESR 900.

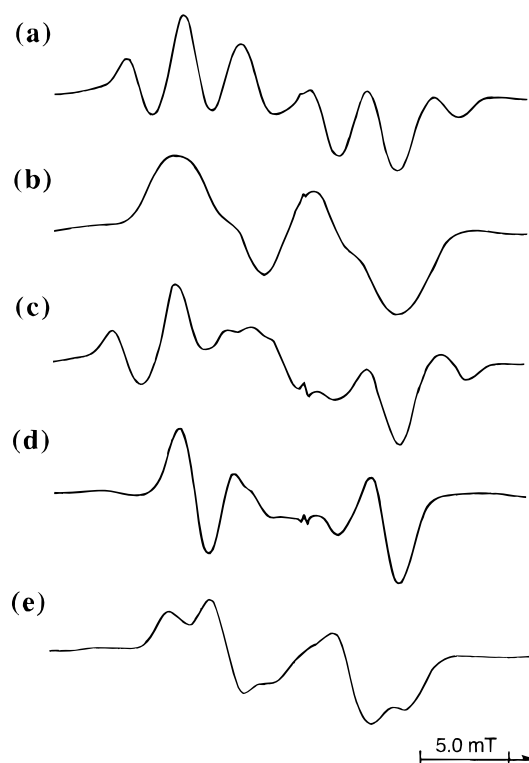


Figure 1. ESR spectra of *c*SiC5 radical cations observed in the CF₃-cC₆F₁₁ matrix at 4.2 K: (a) *c*SiC5⁺, (b) 1,1-Me₂-*c*SiC5⁺, (c) 4,4-Me₂-*c*SiC5⁺, (d) *c*SiC5-2,2,6,6-*d*₄⁺, (e) 1-Me-*c*SiC5-2,2-*d*₂⁺.

TABLE 1: Experimental Isotropic ¹H hf Splittings of the Radical Cations of *c*SiC5 and Its Methyl-Derivatives in the CF₃-cC₆F₁₁ Matrix

radical cation	¹ H hf/mT	T/K
<i>c</i> SiC5 ⁺	7.55 (1H), 2.85 (1H), 3.45 (1H), 2.60 (1H)	4.2
1-Me- <i>c</i> SiC5 ⁺	7.30 (1H), 2.4 (1H), 3.0 (1H), 2.0 (1H)	4.2
1,1-Me ₂ - <i>c</i> SiC5 ⁺ ^a	4.46 (2H), 2.27 (2H)	130
4,4-Me ₂ - <i>c</i> SiC5 ⁺ ^a	5.06 (2H), 3.20 (2H)	4.2

^a The averaged ¹H hf splittings for two pairs of protons, (H_{3e} and H_{5e}) and (H_{2e} and H_{6e}), were observed.

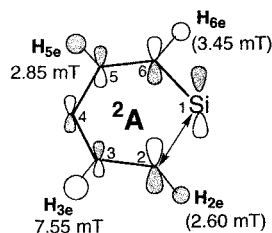
The geometry optimizations of the cation radicals were carried out on a Convex/c3240 computer with Gaussian 90 (UHF/STO-3G) and MOPAC programs at the Information Processing Center, Hiroshima University. The spin densities were evaluated by the INDO MO method for the optimized geometrical structures.^{21,22} The observed temperature dependent ESR spectra were simulated on a personal computer (NEC PC9801 DA) with a program developed by Heinzer.^{23,24} The program uses the equation of motion for the density matrix within the Liouville formalism.

Results and Discussion

1. 4 K ESR Spectra and Asymmetrically Distorted Structure. A. Assignment of Hyperfine Splittings. Figure 1 shows the ESR spectra of (a) *c*SiC5⁺, (b) 1,1-Me₂-*c*SiC5⁺, (c) 4,4-Me₂-*c*SiC5⁺, (d) *c*SiC5-2,2,6,6-*d*₄⁺, and (e) 1-Me-*c*SiC5-2,2-*d*₂⁺ in the CF₃-cC₆F₁₁ matrix recorded at 4.2 K. The experimental hf splittings of the silacyclohexane radical cations are summarized in Table 1. The two selectively deuterated compounds were used to unambiguously assign the experimental hf splittings: ²D hf splittings reduce the corresponding ¹H ones by a factor of *ca.* 6.5, because of the magnetic moment ratio of ¹H to ²D. The 4.2 K ESR spectrum of *c*SiC5⁺ apparently consists of a doublet of triplets with *ca.* 10 mT (1H) and 3 mT (2H). When two methyl groups were substituted for the

hydrogens at the Si atom, the spectrum is changed into a poorly resolved doublet of *ca.* 10 mT (1H) as shown in the spectrum of 1,1-Me₂-cSiC5⁺. The line shape can be simulated with slightly smaller hf splittings than those of cSiC5⁺, but with a wider line width. The result suggests that a small amount of spin density is populated on the hydrogens of the methyl groups. Similarly a substitution of two methyl groups at the C(4) position does not largely change the hf pattern of the original cSiC5⁺ except for poorer resolution at the central band, as shown in the spectrum of 4,4-Me₂-cSiC5⁺. This means the hydrogens at the Si and C(4) positions contributed only to the line width.

On the other hand, the 4.2 K spectrum of cSiC5-2,2,6,6-d₄⁺ consists of a doublet of doublets with hf splittings of 7.55 mT (1H) and 2.85 mT (1H), as shown in Figure 1d. Furthermore the spectrum of 1-Me-cSiC5-2,2-d₂⁺ consists of a doublet of *ca.* 3 mT in addition to the hf pattern of cSiC5-2,2,6,6-d₄⁺, as shown in Figure 1e. These findings suggest that the triplet splitting of *ca.* 3 mT observed for cSiC5⁺ is attributable to two equatorial hydrogens, H_{2e} and H_{6e}, attached to C(2) and C(6). It is well-known that, in both linear and cyclic alkane radical cations, large ¹H hf splittings are generally observed for the hydrogens located at the "trans" position to the σ(C–C) bond(s) with higher spin densities, due to a hyperconjugative mechanism.^{5–10,13–16,25–29} On the basis of the assumption of the σ(Si–C) bonds with higher spin densities than C–C bonds, we can reasonably attribute the observed hf splittings of 7.55 and 2.85 mT to the two equatorial hydrogens, H_{3e} and H_{5e}, at the C(3) and C(5) positions. If the unpaired electron were populated equally on the both Si–C bonds in cSiC5⁺, two pairs of hydrogens, (H_{2e}, H_{6e}) and (H_{3e}, H_{5e}), should give the same hf splitting. To be consistent with the experimental results, therefore, the unpaired electron is suggested to reside preferentially on one of two Si–C bonds. Here we can assume that the Si–C(2) bond has higher spin density than the other one, Si–C(6), *i.e.*, ρ(Si–C(2)) > ρ(Si–C(6)). Then, the hf splittings of H_{3e} and H_{6e} become larger than those of H_{5e} and H_{2e}, respectively, *i.e.*, *a*(H_{3e}) > *a*(H_{5e}) and *a*(H_{6e}) > *a*(H_{2e}). Moreover, taking into account that the Si–C bond length is longer by *ca.* 20% than the C–C bond (see the section of MO calculations), one can easily recognize that *a*(H_{6e}) should become smaller than *a*(H_{3e}), even though the two equatorial hydrogens are located in the trans position to the Si–C(2) bond, *i.e.*, *a*(H_{3e}) > *a*(H_{6e}). Similarly, a relation of *a*(H_{5e}) > *a*(H_{2e}) can be obtained for the other pair of hydrogen splittings at C(5) and C(2). Finally the double-doublet splittings of 7.55 and 2.85 mT observed for cSiC5-2,2,6,6-d₄⁺ can be successfully attributed to H_{3e} and H_{5e}, respectively.



This attribution of the experimental ¹H hf splittings leads us to an asymmetrically distorted C₁ structure of the cSiC5 radical cations in static structure, in which the unpaired electron predominately is present in one of two Si–C bonds, Si–C(2). The Si–C bond with higher spin density is expected to be weaker and elongated. The asymmetrically distorted C₁ structure derived from the present experimental results was theoretically supported, as mentioned in the next section.

B. Origin of the Structural Distortion. The structural distortion can be explained by using second-order Jahn–Teller

theory (pseudo-Jahn–Teller effect).^{30,31} The theory predicts that the vibronic–electronic coupling, which is inversely proportional to the energy difference between the ground and electronic excited states, can induce the structural distortion of molecules.

Based on the second-order perturbation theory, the energy of the radical cation in the ground electronic state is given by a following equation (1).

$$E = E_0 + Q \left\langle \psi_0 \left| \frac{\partial U}{\partial Q} \right| \psi_0 \right\rangle + \frac{Q^2}{2} \left\langle \psi_0 \left| \frac{\partial^2 U}{\partial Q^2} \right| \psi_0 \right\rangle + \sum_k \frac{\left[Q \left\langle \psi_0 \left| \frac{\partial U}{\partial Q} \right| \psi_k \right\rangle \right]^2}{(E_0 - E_k)} \quad (1)$$

where E_0 is the energy without distortion, Q is the displacement of the normal coordinate from the original position, U is the nuclear–nuclear and nuclear–electronic potential energy, and ψ_0 and ψ_k are the wave functions for the ground electronic state and an electronic excited state, respectively. For an asymmetric displacement the second term in the equation is zero because of being an odd function, while the third and the fourth terms are always positive and negative, respectively. Therefore, whether the asymmetrically distorted structure is preferable or not is determined by a sum of the two terms; that is, when the sum is positive or negative, the symmetrical or the asymmetrical structure is energetically preferable, respectively. The absolute value of the fourth term is inversely proportional to the energy difference between the electronic ground state and the lower lying electronic excited states. In case where the energy difference is smaller than several electronvolts (eV), as for the present radical cations, the fourth term predominates over the third term so as to make the asymmetrical C₁ structure more stable than the symmetrical structure.

In a variety of allyl type radicals, for example, the structural distortion has been discussed in terms of the second-order Jahn–Teller effect.^{30–32} Recently, a structural distortion similar to the present one has been reported for the σ type radical cations of *n*-propane, *n*-pentane, their methyl-substitutions with C_s symmetry, and norbornane by Toriyama and Okazaki.^{13–16} They have claimed that the distorted structure due to the second-order Jahn–Teller effect is stabilized by the matrix used, so that the distortion becomes larger in the matrix with the larger dipole moment. Furthermore, M. J. Shephard and M. N. Paddon-Row have reported the MO calculations on norbornane⁺ to support that the structural distortion is caused by the matrix used.³³ However, in the present study, almost the same structural distortion was observed for the cSiC5⁺ system when the matrix was changed from cC₆F₁₂ to CFCl₂CFCl₂, CF₂CICFCl₂, CF₃-CCl₃, CF₂CICF₂Cl, and CF₃-cC₆F₁₁. This observation can originate from the intrinsic nature of cSiC5⁺; the matrix can only play a role of perturbation. Furthermore, we add to note that, in our previous studies^{7–10,25,26} on cyclohexane methyl-derivatives⁺ and 1-methylsilacyclohexane⁺, similar structural distortions have been clearly observed in the cC₆F₁₂ matrix which have been expected not to affect the structure of solute radical cation rather than in the other halocarbone matrix because of its soft spongy structure with large vacancies. The details of the vacancies in the solid cC₆F₁₂ have been recently studied using the positron annihilation method by one of the present authors.³⁴

C. MO Calculations. Geometry optimization of cSiC5⁺ was performed for two different structures, C₁ and C_s, using the *ab-initio* MO method (Gaussian 90/STO-3G basis set). The

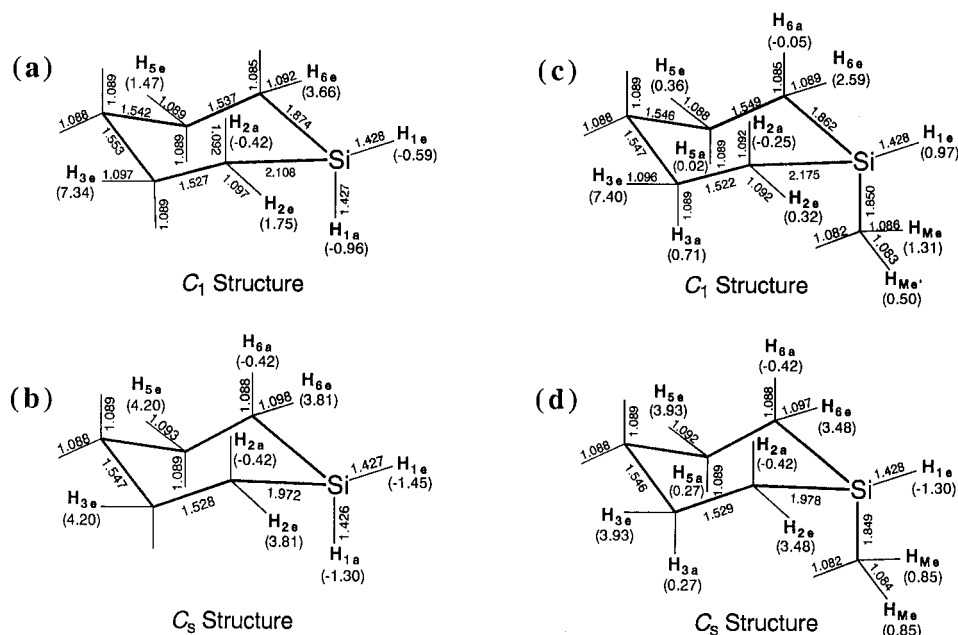


Figure 2. Optimized C_1 and C_2 geometrical structures of $cSiC_5^+$ and 1-Me- $cSiC_5^+$, a and b, c, and d, respectively, calculated by using the *ab-initio* MO method at the UHF/STO-3G level of Gaussian 90. The values in parentheses are the isotropic 1H hf splittings evaluated by the INDO MO method for each structure. The bond lengths are in angstroms.

optimized bond lengths are summarized in Figure 2a,b for the C_1 and C_s structures, respectively. Consistently with the experiments the calculations resulted in the C_1 structure, which is more stable by 0.33 eV than C_s in total energy.

For the C_1 structure a longer Si-C bond is calculated to be 2.108 Å, 13% elongated with respect to the "normal" Si-C bond, 1.867 Å, of the neutral molecule. The calculations show that all the bond lengths including the other Si-C bond remain almost unchanged after one-electron oxidation. This means that only the position of the Si atom is selectively shifted by changing from the original C_s structure to C_1 .

The 1H hf splittings were evaluated by the INDO-MO method for the optimized C_1 structure (in parentheses in Figure 2a). The calculated hf splittings for the four equatorial hydrogens, H_{3e}, H_{5e}, H_{2e}, and H_{6e}, are compared with the experimental ones as follows: 7.34 mT (calc) *vs* 7.55 mT for H_{3e}, 1.47 mT (calc) *vs* 2.85 mT for H_{5e}, 3.66 mT (calc) *vs* 3.45 mT for H_{6e}, and 1.75 mT (calc) *vs* 2.60 mT for H_{2e}. The rather good agreement was obtained between the calculated hf splittings for the distorted geometry and the experimentally observed ones. It is known that UHF calculations, especially with small basis sets, sometimes predict artificial symmetry breaking also in cases which from high-level calculations and experiment are known to have a higher symmetry.³⁵ However, the present calculations give strong support for the experimental results. Thus, an asymmetrically distorted C_1 structure of $cSiC_5^+$ was concluded both experimentally and theoretically.

It is interesting to see how the degree of distortion is affected by introducing one or two methyl groups to the Si atom. The optimized geometrical structures for 1-Me- $cSiC_5^+$ with C_1 and C_s symmetry are shown in Figure 2c,d, respectively. For the distorted C_1 structure, the two Si-C bond lengths were evaluated to be 2.175 and 1.862 Å; note that the bond lengths are 2.108 and 1.874 Å for nonmethylated $cSiC_5^+$ with the same symmetry. Thus, the distortion becomes slightly larger by introducing one methyl group to the Si atom. The calculations are consistent with the experimental results: taking the ratio of hf splittings of $a(H_{3e})$ to $a(H_{5e})$ as an experimental measure of the distortion, we have a slightly smaller value of 2.6 ($=7.55/2.85$) for the $cSiC_5^+$ than that for the 1-Me- $cSiC_5^+$, 3.0 ($=7.3/2.4$).

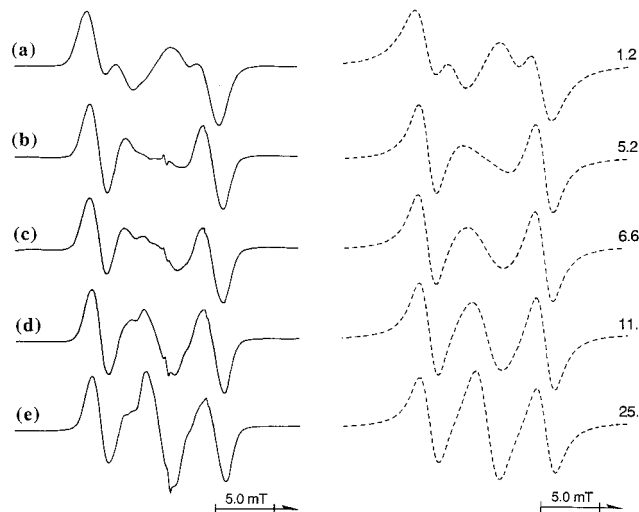
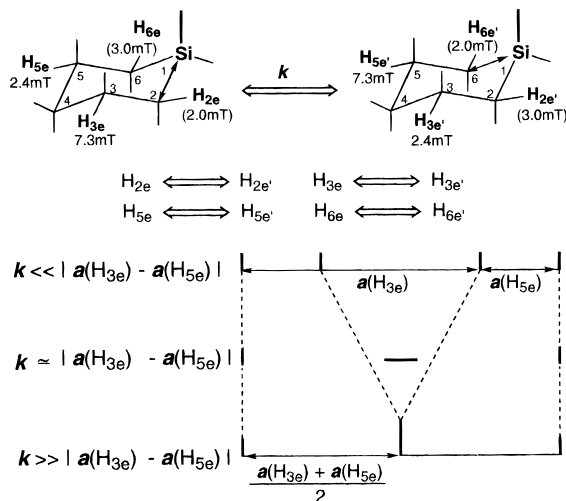


Figure 3. Temperature dependent ESR spectra of 1-Me- $cSiC_5$ -2,2,6,6- d_4^+ observed in CF_3 - cC_6F_{11} matrix: (a) 4.2 K, (b) 77 K, (c) 110 K, (d) 130 K, (e) 140 K. The dotted lines in the right column are the simulated spectra together with the exchange rate constant, k (in 10^7 s $^{-1}$), employed in the calculations.

2. Temperature Dependent ESR Spectra and the Line Shape Analysis. *A. Experimental Spectra.* Figure 3 shows the temperature dependent ESR line shapes of 1-Me- $cSiC_5$ -2,2,6,6- d_4^+ in the CF_3 - cC_6F_{11} matrix. The spectra were observed in a wide temperature range from 4.2 to 140 K. The 4.2 K spectrum consisted of double doublets with hf splittings of 7.3 and 2.4 mT. The inner doublet was less intense than the outer one and almost disappeared at 77 K. Upon further increasing temperature, a singlet newly appeared at the central position and its intensity increased with temperature. At 140 K the spectrum became a triplet of *ca.* 4.9 mT with the relative intensity close to a binomial one (1:2:1). This suggests that the two hydrogens, H_{3e} and H_{5e}, attached at C(3) and C(5) become magnetically equivalent at higher temperature. The spectral change was reversible with temperature, and the total hf splitting remained constant below 140 K. A similar temperature dependency of the ESR spectra was observed for $cSiC_5$ -2,2,6,6- d_4^+ in the cC_6F_{12} matrix.

B. Selective Bond Length Alternation between Two Adjacent Si-C Bonds. The ESR spectral line shape change as shown in Figure 3 is characteristic of a hf averaging process due to an interchange of two hydrogens with 7.3 and 2.4 mT. The following dynamic model is proposed to explain the observed temperature dependent ESR line shapes. As mentioned in the previous section, 1-Me-cSiC5⁺ takes an asymmetrically distorted structure with one Si-C bond elongated. Then, 1-Me-cSiC5⁺ has two energetically equivalent mirror image structures, one with the Si-C(2) bond elongated and the other with the Si-C(6) bond elongated. Here we can assume an intramolecular hydrogen exchange between the two structures. It is schematically presented how ¹H hf splittings of 7.3 and 2.4 mT are averaged out by such an intramolecular exchange process below.



The lower diagram shows how the ESR line shapes depend on exchange rate, k (s^{-1}). The 4.2 K spectrum of 1-Me-cSiC5-2,2,6,6- d_4^+ shows the weaker inner doublet compared to the outer, as mentioned already. This observation is reasonably explained by assuming that the hf splittings of H_{3e} and H_{5e} have been already partially averaged by the intramolecular exchange process with a slightly smaller rate constant, k (s^{-1}), than the hf splitting difference in the two hydrogens, $a(H_{3e}) - a(H_{5e}) = 1.3 \times 10^7$ (s^{-1}). With a k value nearly equal to the difference of two hf splittings, the inner doublet should disappear, as observed around 77 K. On further increasing temperature, a new singlet appears at the central position and its intensity grows, suggesting further increase in rate constant.

C. Spectral Line Shape Analysis. The temperature dependent ESR spectral line shapes observed for a series of silacyclohexane radical cations in the CF_3 - cC_6F_{11} matrix were simulated on the basis of the intramolecular exchange model. The simulated spectra best fitted to the experimental ones are shown with dotted lines in Figures 3, 4, and 5. The rate constants, k (s^{-1}), employed for the simulation are given on the shoulder of each calculated spectrum.

For simplicity we start with the 1-Me-cSiC5-2,2,6,6- d_4 radical cation. Interestingly the 4.2 K spectrum was simulated with a rate constant of $k = 1.2 \times 10^7$ s^{-1} , but not with the assumption of rigid limit. The simulations successfully reproduce the disappearing of the inner doublet and the increasing of the central singlet as observed in the course of warming the sample. Thus we could demonstrate that the spectral change is associated with averaging of two hf splittings, $a(H_{3e})$ and $a(H_{5e})$. Note that the values of 1.1 and 0.8 mT were used as the line width, ΔH_{msl} , for simulating the experimental spectra recorded at 4.2–60 K and above 60 K, respectively. Similarly the temperature

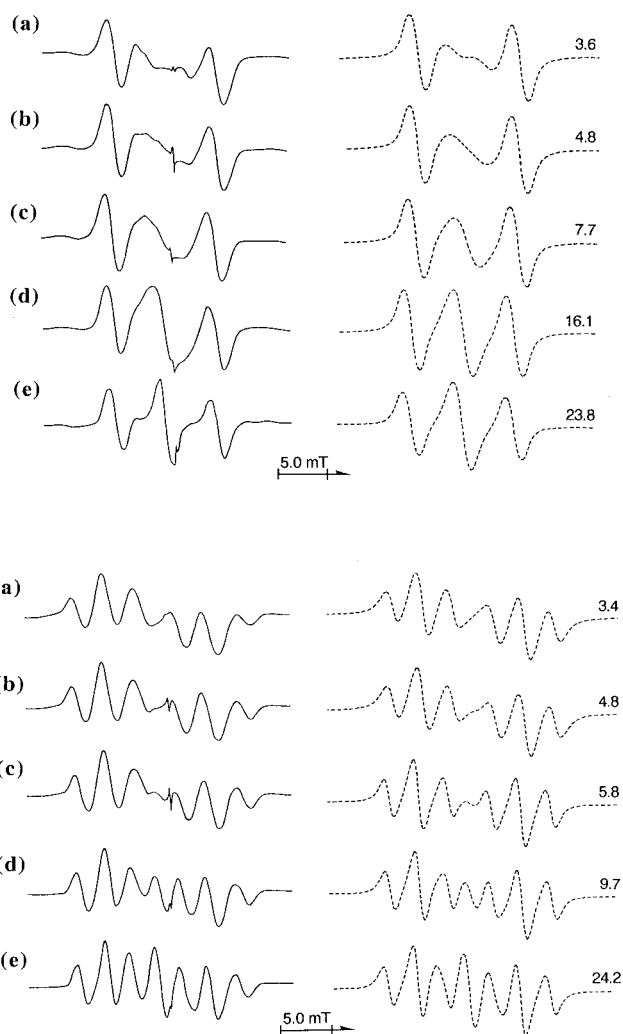


Figure 4. Temperature dependent ESR spectra of $cSiC5$ -2,2,6,6- d_4^+ (upper) and $cSiC5^+$ (lower) observed in the CF_3 - cC_6F_{11} matrix: (a) 4.2 K, (b) 40 K, (c) 77 K, (d) 110 K, (e) 130 K. The dotted lines in the right column are the simulated spectra together with the rate constant k (in 10^7 s^{-1}) employed.

dependent spectra of the radical cation observed in the cC_6F_{12} matrix were also successfully simulated.

Now we move on to the simulation of $cSiC5^+$ (Figure 4). In order to simulate the associated temperature dependent spectra, we have to know the hf splittings of $a(H_{2e})$ and $a(H_{6e})$ in the rigid state in addition to the $a(H_{3e})$ and $a(H_{5e})$ derived from the 4.2 K spectrum of $cSiC5$ -2,2,6,6- d_4^+ . Experimentally, however, only the averaged value of $a(H_{2e})$ and $a(H_{6e})$ can be known. Therefore we carried out the simulations using $a(H_{2e})$ and $a(H_{6e})$ as variable parameters. After many trial calculations we found that $a(H_{2e}) = 2.60$ mT and $a(H_{6e}) = 3.45$ mT gave the best fit simulation spectra over the temperature range studied.

As shown in Figure 5 (lower), the 1-Me-cSiC5-2,2- d_2 radical cation gave similar temperature dependent ESR spectra, which could be also successfully analyzed by using the same intramolecular dynamic model.

D. Arrhenius Plot. Arrhenius plots of the rate constants, k (s^{-1}), for the intramolecular dynamics are shown in Figure 6. The rate constants were evaluated by simulations of the temperature dependent spectral line shapes of $cSiC5^+$ and 1-Me- $cSiC5^+$ and their selectively deuterated cations in the CF_3 - cC_6F_{11} matrix. The plots show a nonlinear relationship over the temperature range 4.2–130 K for all silacyclohexane radical cations studied. Assuming a linear relationship in the higher temperature region between 60 and 130 K, an activation energy

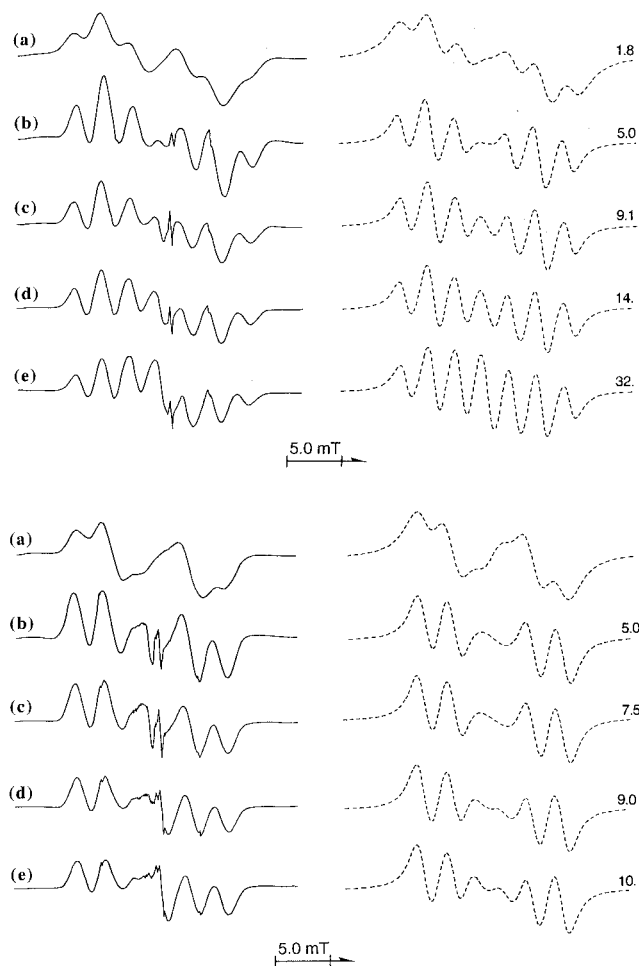


Figure 5. Temperature dependent ESR spectra of 1-Me-*c*SiC5⁺ (upper) and 1-Me-*c*SiC5-2,2-*d*₂⁺ (lower) observed in the CF₃-*c*C₆F₁₁ matrix: (a) 4.2 K, (b) 77 K, (c) 110 K, (d) 130 K, (e) 140 K. The dotted lines in the right column are the simulated spectra together with the rate constant *k* (in 10⁷ s⁻¹) employed.

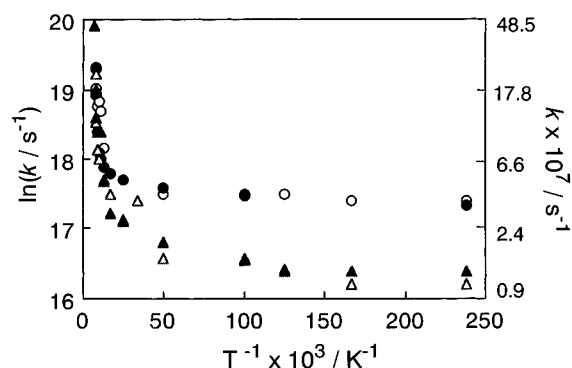
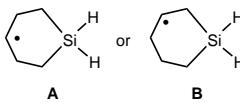
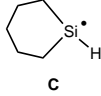
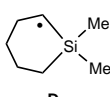


Figure 6. Arrhenius plots of the rate constant *k* evaluated by the simulation of the temperature dependent ESR spectra observed for *c*SiC5 radical cations in the CF₃-*c*C₆F₁₁ matrix: (○) *c*SiC5-2,2,6,6-*d*₄⁺, (●) *c*SiC5⁺, (△) 1-Me-*c*SiC5-2,2,6,6-*d*₄⁺, (▲) 1-Me-*c*SiC5⁺.

of *ca.* 0.3 kcal/mol was evaluated. Below 40 K, the rate constants were almost independent of temperature: $k = 3.6 \times 10^7$ s⁻¹ for the *c*SiC5⁺ system and $k = 1.2 \times 10^7$ s⁻¹ for the 1-Me-*c*SiC5⁺ system. Introducing one methyl group to the Si atom, the rate constant was reduced to one third of the original value. No appreciable deuterium effect on the rate constant was observed for *c*SiC5-2,2,6,6-*d*₄⁺ or 1-Me-*c*SiC5-2,2,6,6-*d*₄⁺.

The nonlinear Arrhenius plots are characteristic of a quantum mechanical tunneling effect.³⁶ In the present case the dynamics is characterized by a symmetric double-well potential surface and can be explained by assuming that the state is settled at the

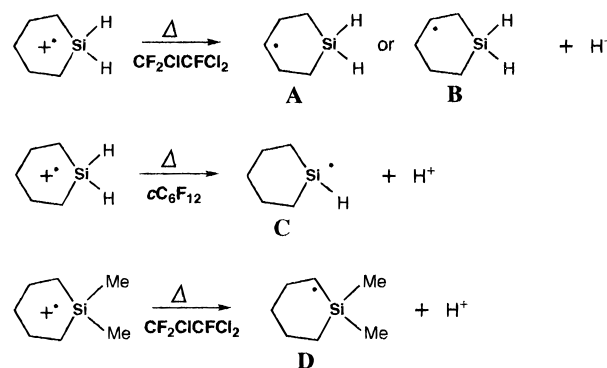
TABLE 2: Experimental Isotropic ¹H hf Splittings of the Neutral Radicals Generated by the Deprotonation from *c*SiC5 Radical Cations at Elevated Temperatures

radical	matrix	¹ H hf/mT	T/K
 A or B	CF ₂ CICFCl ₂	2.20 (1H _α), 3.60 (4H _β)	120
 C	<i>c</i> C ₆ F ₁₂	1.93 (1H _α), 1.70 (2H _β), 0.58 (2H _γ)	162
 D	CF ₃ - <i>c</i> C ₆ F ₁₁ CF ₂ CICFCl ₂	1.9 (1H _α) 2.08 (1H _α), 4.64 (1H _β), 1.59 (1H _γ)	160 120

zero-vibrational level of one of the two wells and the heavy atom of Si moves to the another side through the barrier, for example, with a rate constant of *ca.* 36 MHz for *c*SiC5-2,2,6,6-*d*₄⁺ at 4.2 K. Thus, we propose that the dynamics might take place preferably via the quantum mechanical tunneling effect and not thermodynamically, especially in the low-temperature region. Here we note several references^{36–40} suggesting the spectroscopic evidence of heavy particle tunneling concerned with the intramolecular rearrangements in organic molecules, which include the automerization of cyclobutadiene.^{37–39} Further theoretical investigations are called for predicting the potential surface and tunneling probabilities for the intramolecular dynamics of *c*SiC5⁺.

3. Thermal Reaction. The *c*SiC5 radical cations were converted into neutral radicals by a site selective deprotonation at elevated temperature. The site preference was found to depend on the number of methyl groups at the Si atom and the matrix used. The observed neutral radicals and hf splittings are summarized in Table 2.

The ESR spectrum of *c*SiC5⁺ in the CF₂CICFCl₂ matrix was irreversibly changed into a quintet of doublets with hf splittings of 3.60 mT (4H) and 2.20 mT (1H) upon warming above 120 K. The ESR spectrum can be assigned to a neutral radical (species A or B) having a radical center at C(3) or C(4) position, respectively.



On the other hand, in the *c*C₆F₁₂ matrix, *c*SiC5⁺ was irreversibly changed into the radical with 12 lines consisting of a doublet of triple-triplets with hf splittings of 1.93 mT (1H), 1.70 mT (2H), and 0.58 mT (2H) at 162 K. The 1.70 mT splitting is close to the α -hydrogen (1.9 mT) of (CH₃)₂HSi[•] reported by Krucic *et al.*⁴¹ Thus, the observed spectrum is attributed to the neutral radical with a radical center at the Si atom. We conclude that in the *c*C₆F₁₂ matrix the deprotonation occurred preferentially from the =SiH₂ to give species C. The site selectivity for the radical formation is almost 100% since

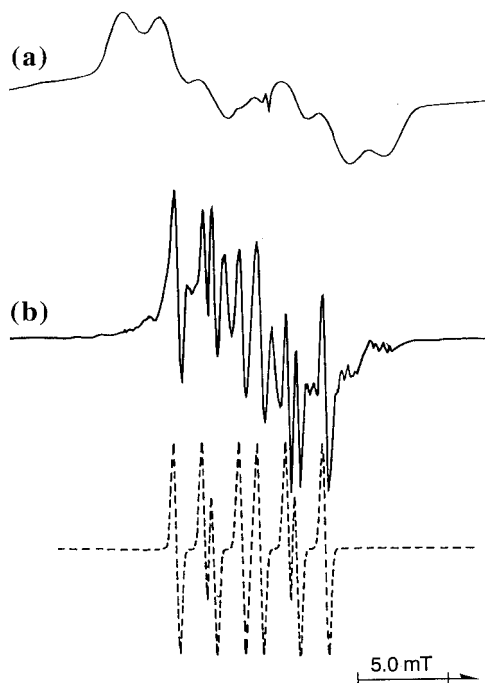


Figure 7. (a) ESR spectrum of $1,1\text{-Me}_2\text{-cSiC}_5^+$ observed at 77 K in the $\text{CF}_2\text{ClCFCl}_2$ matrix. (b) ESR spectrum of a neutral radical formed by the deprotonation from $1,1\text{-Me}_2\text{-cSiC}_5^+$ at 120 K in the same matrix. The dotted line is a simulated spectrum using the isotropic ^1H hf splittings of 2.08 mT (1H), 4.64 mT (1H), and 1.59 mT (1H).

other radical species were not detected. Note that a similar ESR spectrum, but with poor resolution, was observed in the $\text{CF}_3\text{-cC}_6\text{F}_{11}$ matrix above 140 K.

$1,1\text{-Me}_2\text{-cSiC}_5^+$ was changed into a six-line spectrum with hf splittings of 2.08 mT (1H), 4.64 mT (1H), and 1.59 mT (1H) in $\text{CF}_2\text{ClCFCl}_2$ at 120 K (Figure 7). The ESR spectrum can be assigned to species **D**, which was formed by the site selective deprotonation at the methylene groups next to the Si atom.

Several mechanisms have been proposed to explain the deprotonation reaction for the radical cation of saturated hydrocarbons formed in solid solutions at low temperatures: ion–molecule reaction, charge neutralization reaction, and so on.²⁰ For example, it has been reported that the deprotonation occurs predominately at the hydrogen with highest spin density for some alkane radical cations.⁴² However, we have already pointed out that the deprotonation from alkane radical cations cannot be fully explained by such a mechanism, as exemplified by the radical cations of cyclohexanes⁺.⁴³ In the case of cSiC_5 and $1,1\text{-Me}_2\text{-cSiC}_5$ radical cations we cannot find any correlation between the site at which the deprotonation occurs and the hf splitting of the hydrogen. The dissociation energy of H from SiH_2 in a sila-alkane is smaller by a few kcal mol^{-1} than that from CH_2 in an alkane. This suggests that formation of the silyl radical might be energetically more favorable. The solvating energy and the orientation of the radical molecule in the matrix can also be important factors to explain the observed high geoselective reaction.

Concluding Remarks

We presented experimental ESR evidence showing the asymmetrically distorted C_1 structure of cSiC_5^+ in $\text{CF}_3\text{-cC}_6\text{F}_{11}$ and cC_6F_{12} matrices, in which the unpaired electron resides preferentially on a particular Si–C bond. The structural distortion can be caused by the pseudo-Jahn–Teller effect, which is in agreement with Toriyama.¹⁶ However, the present results show that the matrix does not play a critical role for the

structural distortion of cSiC_5^+ . In fact the structural distortion similar to that of silacyclohexanes⁺ has been observed not only for Me-cC_6^+ and $1,1\text{-Me}_2\text{-cC}_6^+$ ^{7–10} but also for $1,c_2,c_3\text{-Me}_3\text{-cC}_6^+$, $1,r_2,c_3\text{-Me}_3\text{-cC}_6^+$,²⁷ cSiC_4^+ , 1-Me-cSiC_4^+ , $1,1\text{-Me}_2\text{-cSiC}_4^+$, Me-cC_5^+ , $1,1\text{-Me}_2\text{-cC}_5^+$, Et_2Si^+ , Et_2SiMe^+ , $\text{Et}_2\text{SiMe}_2^+$, and Et_4Si^+ ^{44–47} in our group. Thus, we believe the decrease in symmetry with one-electron oxidation is an intrinsic nature of alkane radical cations whose parent molecules have some symmetrical elements such as C_s , C_2 , and C_{2v} in the geometrical structure, even though they are not Jahn–Teller active. Note that the above arguments do not completely rule out any possibility of structural distortion induced by the matrix. As expected for some alkane radical cations with a rather weak pseudo-Jahn–Teller effect, the matrix might play some role to stabilize the structural distortion.

The temperature dependent ESR spectra were observed for the silacyclohexane radical cations in the temperature range between 4 and 130 K. The ESR spectral line shapes were successfully analyzed by assuming intramolecular dynamics, *i.e.*, the selective Si–C bond length alternation between two magnetically equivalent distorted C_1 structures. Furthermore, Arrhenius plots of the rate constants were found to be nonlinear over the temperature range. It was found that, especially below 40 K, the rates were almost independent of temperature. The results strongly suggest that the dynamics can take place due to the quantum mechanical tunneling effect.

Upon increasing temperature above 140 K, the cSiC_5 radical cations were converted into the neutral radicals via geoselective deprotonations. The sites at which the deprotonation preferentially occurs depended on not only the matrices used but also the position and number of methyl groups introduced.

Acknowledgment. The authors are indebted to Mr. F. Yasutake for assistance in the preliminary experiments. The author also thanks Prof. M. Ishikawa and Dr. J. Ohshita for valuable advice in synthesis of the deuterated silacyclohexanes. The present study was partially supported by the JSPS program for Supporting University Industry Cooperative Research Project and a Subsidy of Science Research of the Japanese Ministry of Education (Grant No. 08240105).

References and Notes

- (1) Iwasaki, M.; Toriyama, K.; Nunome, K. *J. Am. Chem. Soc.* **1981**, *103*, 3591.
- (2) Toriyama, K.; Nunome, K.; Iwasaki, M. *J. Phys. Chem.* **1981**, *85*, 2149.
- (3) Nunome, K.; Toriyama, K.; Iwasaki, M. *Tetrahedron* **1986**, *42*, 6315.
- (4) Iwasaki, M.; Toriyama, K.; Nunome, K. *Faraday Discuss. Chem. Soc.* **1984**, *75*, 19.
- (5) Toriyama, K.; Nunome, K.; Iwasaki, M. *J. Chem. Phys.* **1982**, *77*, 5891.
- (6) Shiotani, M.; Yano, A.; Ohta, N.; Ichikawa, T. *Chem. Phys. Lett.* **1988**, *147* (1), 38.
- (7) Shiotani, M.; Ohta, N.; Ichikawa, T. *Chem. Phys. Lett.* **1988**, *149*, 185.
- (8) Lindgren, M.; Shiotani, M.; Ohta, N.; Ichikawa, T.; Sjöqvist, L. *Chem. Phys. Lett.* **1989**, *161*, 127.
- (9) Sjöqvist, L.; Lindgren, M.; Lund, A.; Shiotani, M. *J. Chem. Soc., Faraday Trans.* **1990**, *86*, 3377.
- (10) Shiotani, M.; Lindgren, M.; Ohta, N.; Ichikawa, T. *J. Chem. Soc., Perkin Trans. 2* **1991**, 711.
- (11) Lide, D. R., Ed. *CRC Hand Book of Chemistry and Physics*, 73rd ed.; CRC Press Inc.: Cleveland, OH, 1992.
- (12) Ouellette, R. J. *J. Am. Chem. Soc.* **1974**, *96*, 2421.
- (13) Toriyama, K. *Chem. Phys. Lett.* **1991**, *177*, 39.
- (14) Toriyama, K.; Okazaki, M.; Nunome, K. *J. Chem. Phys.* **1991**, *95*, 3955.
- (15) Toriyama, K.; Okazaki, M. *J. Phys. Chem.* **1992**, *96*, 6986.
- (16) Okazaki, M.; Toriyama, K. *J. Phys. Chem.* **1993**, *97*, 8212.
- (17) Nguyen, B. T.; Cartledge, F. K. *J. Org. Chem.* **1986**, *51*, 2206.
- (18) Symons, M. C. R. *Chem. Soc. Rev.* **1984**, 393.

- (19) Shiotani, M. *Magn. Reson. Rev.* **1987**, *12*, 333.
(20) Lund, A.; Shiotani, M. *Radical Ionic Systems*; Kluwer Academic Publishers: Dordrecht, 1991.
(21) Pople, J. A.; Beveridge, D. L.; Dobosh, P. A. *J. Chem. Phys.* **1957**, *47*, 2026.
(22) Veillard, A.; Berthier, G. *Theor. Chim. Acta* **1965**, *3*, 213.
(23) Heinzer, J. *Mol. Phys.* **1971**, *22*, 167.
(24) *QCPE Program*, No. 209, Indiana University, 1972.
(25) Shiotani, M.; Komaguchi, K.; Ohshita, J.; Ishikawa, M.; Sjoqvist, L. *Chem. Phys. Lett.* **1992**, *188*, 93.
(26) Komaguchi, K.; Shiotani, M.; Ishikawa, M.; Sasaki, K. *Chem. Phys. Lett.* **1992**, *200*, 580.
(27) Shiotani, M.; Lindgren, M.; Ichikawa, T. *J. Am. Chem. Soc.* **1990**, *112*, 967.
(28) Lindgren, M.; Matsumoto, M.; Shiotani, M. *J. Chem. Soc., Perkin Trans. 2* **1992**, 1397.
(29) Shiotani, M.; Matsumoto, M.; Lindgren, M. *J. Chem. Soc., Perkin Trans. 2* **1993**, 1995.
(30) Pearson, R. G. *J. Am. Chem. Soc.* **1969**, *91*, 1252.
(31) Pearson, R. G. *J. Am. Chem. Soc.* **1969**, *91*, 4947.
(32) Feller, D.; Davidson, E. R.; Borden, W. T. *J. Am. Chem. Soc.* **1984**, *106*, 2513.
(33) Shephard, M. J.; Paddon-Row, N. *J. Phys. Chem.* **1995**, *99*, 3101.
(34) Ito, Y.; Mohamed, H. F. M.; Shiotani, M. *J. Phys. Chem.* **1996**, *100*, 14161.
(35) Feller, D.; Huyser, E. S.; Borden, W. T.; Davidson, E. R. *J. Am. Chem. Soc.* **1983**, *105*, 1459.
(36) Benderskii, V. A.; Makarov, D. E.; Wight, C. A. *Chemical Dynamics at Low Temperatures, Advances in Chemical Physics, Volume LXXXVIII*; John Wiley and Sons, Inc.: New York, 1994.
(37) Whitman, D. W.; Carpenter, B. K. *J. Am. Chem. Soc.* **1982**, *104*, 6473.
(38) Dewar, M. J. S.; Merz, K. M.; Stewart, J. J. P. *J. Am. Chem. Soc.* **1984**, *106*, 4040.
(39) Carsky, P.; Bartlett, R. J.; Fitzgerald, G.; Noga, J.; Spirko, V. *J. Chem. Phys.* **1988**, *89*, 3008.
(40) Okuyama, K.; Kakinuma, T.; Fujii, M.; Mikami, N.; Ito, M. *J. Phys. Chem.* **1986**, *90*, 3948.
(41) Krusic, P. J. *J. Am. Chem. Soc.* **1969**, *91*, 3938.
(42) Toriyama, K.; Nunome, K.; Iwasaki, M. *J. Phys. Chem.* **1986**, *90*, 6836.
(43) Shiotani, M.; Lindgren, M.; Takahashi, F.; Ichikawa, T. *Chem. Phys. Lett.* **1990**, *170*, 201.
(44) Lindgren, M.; Komaguchi, K.; Shiotani, M.; Sasaki, K. *J. Phys. Chem.* **1994**, *98*, 8331.
(45) Komaguchi, K.; Shiotani, M.; Ishikawa, M. *Japanese ESR Symposium (32nd)* **1993**, *32*, 41.
(46) Marutani, T.; Komaguchi, K.; Shiotani, M. *Japanese Radiation Chemistry Symposium (35th)* **1992**, *35*, 161.
(47) Shiotani, M. Unpublished data.